Formation of new chromosomes as a virulence mechanism in yeast *Candida glabrata*

Silvia Poláková[a], Christian Blume[a], Julián Álvarez Zárate[a], Marek Mentel[a,b], Dorte Jørck-Ramberg[b], Jørgen Stenderup[c], and Jure Piškur[a,b,1]

[a]Department of Cell and Organism Biology, Lund University, SE-22362 Lund, Sweden; [b]Department of Systems Biology, Technical University of Denmark, DK-2800 Lyngby, Denmark; and [c]Department of Clinical Microbiology, Regionshospitalet Herning, DK-7400 Herning, Denmark

Edited by John A. Carbon, University of California, Santa Barbara, CA, and approved January 9, 2009 (received for review September 30, 2008)

In eukaryotes, the number and rough organization of chromosomes is well preserved within isolates of the same species. Novel chromosomes and loss of chromosomes are infrequent and usually associated with pathological events. Here, we analyzed 40 pathogenic isolates of a haploid and asexual yeast, *Candida glabrata*, for their genome structure and stability. This organism has recently become the second most prevalent yeast pathogen in humans. Although the gene sequences were well conserved among different strains, their chromosome structures differed drastically. The most frequent events reshaping chromosomes were translocations of chromosomal arms. However, also larger segmental duplications were frequent and occasionally we observed novel chromosomes. Apparently, this yeast can generate a new chromosome by duplication of chromosome segments carrying a centromere and subsequently adding novel telomeric ends. We show that the observed genome plasticity is connected with antifungal drug resistance and it is likely an advantage in the human body, where environmental conditions fluctuate a lot.

chromosome rearrangements | evolution | genome stability | pathogenicity | segmental duplications

Gene content and chromosome organization differ from species to species. However, in most eukaryotes, including yeasts, the chromosome structure seems to be well preserved within the members of the same species, where regular sexual cycles help to preserve the genome organization. Genomic instability, including aneuploidy and changes in chromosome structure, is apparently very low and usually associated with pathological events, for example, in cancer development in mammals (1, 2). In sexual species, chromosomal rearrangements can lead to sexual isolation and subsequent speciation (3). *Candida glabrata*, which is the second most prevalent yeast pathogen in humans, has been traditionally classified as a haploid and asexual organism. The genome of one strain has been recently sequenced (4), and the genome structure now provides a tool for understanding *C. glabrata* virulence. Rapid changes in *C. glabrata* genomic organization have been reported in many clinical studies (5–7). In addition, isolates from one patient often exhibit 2 or 3 different karyotypes and during infection the chromosome pattern can change within a few days (6). So far the mechanisms behind the genome flexibility, adaptability, and virulence have been only poorly understood in this yeast.

Results and Discussion

Clinical Isolates of *C. glabrata*. We analyzed 40 clinical isolates of *C. glabrata* obtained from Danish patients that were randomly selected from the Danish Statens Serum Institute collection (Table S1). All isolates were confirmed to belong to the *C. glabrata* species by sequencing of the D1/D2 domain of *LSU* rDNA and partial sequencing of mitochondrial *SSU* rDNA (Table S2). In addition, a more detailed phylogenetic relationship among isolates was resolved by sequencing and analysis of the sequences belonging to the fast evolving intergenic spacer (IGS) region between the nuclear genes *CDH1* and *ERP6* on chromosome A (see Fig. 2 and Table S2). The variability among strains for this sequence was <2%.

Karyotypes Vary A Lot. The yeast chromosomes were separated by pulsed-field gel electrophoresis (PFGE). Although the strains, based on the 3 sequenced loci, show little sequence variability, their karyotypes were quite variable. The separated chromosomes were hybridized with 93 single-gene probes and 1 multigene probe corresponding to *LSU* rDNA (Table S3). In the initial mapping we used 2 unique probes per chromosome: 1 from the middle (labeled "m") and 1 from near a chromosome end (labeled "er" for right or "el" for left) (Table S3 and Figs. S1 and S2). The karyotype of *C. glabrata* CBS 138, the sequenced strain, was used as a reference, and the expected position of the probes confirmed by hybridization. The largest chromosome size polymorphisms were associated with either translocations of chromosomal arms or interchromosomal duplications involving 12 of 13 chromosomes (Fig. S2). The two largest chromosomes, M and L, contain the rDNA locus and showed pronounced variability in size without any translocations detected. A copy number variation of the rDNA cluster or intrachromosomal segmental duplications/deletions could explain the observed polymorphism. In a few cases, the *LSU* rDNA probe also hybridized to smaller chromosomes, probably as a result of recent translocation events.

Molecular Mechanisms Behind Rearrangements. Fifteen strains, covering chromosome changes of all 40 isolates, were selected for further mapping, using close to 100 gene probes (Table S3), to understand the organization of centromeres, telomeres, chromosome number, some segmental duplications, and translocations (Fig. 1 and Table S4). Seven reciprocal and 4 nonreciprocal translocations were observed, identifying all but CBS 138 chromosome C to be involved in these rearrangements. Note that if the translocation involved a chromosome end <20 kb, our approach could not classify it as reciprocal. Three of these nonreciprocal translocations were found in several strains, likely representing an early event during the evolutionary history of *C. glabrata* (Fig. 2). However, the origin of these translocation events is much younger than the chromosomal translocations reported for the *Saccharomyces sensu stricto* sister species (8).

Interchromosomal duplications represent a subclass of translocations. Five events, where a duplicated chromosomal segment was translocated to another chromosome or fused with another duplicated segment originating from a different chromosome,

Author contributions: S.P. and J.P. designed research; S.P., C.B., J.Á.Z., M.M., and D.J.-R. performed research; J.S. contributed new reagents/analytic tools; S.P., C.B., D.J.-R., and J.P. analyzed data; and S.P. and J.P. wrote the paper.

The authors declare no conflict of interest.

This article is a PNAS Direct Submission.

Freely available online through the PNAS open access option.

[1]To whom correspondence should be addressed. E-mail: jure.piskur@cob.lu.se.

This article contains supporting information online at www.pnas.org/cgi/content/full/0809793106/DCSupplemental.

www.pnas.org/cgi/doi/10.1073/pnas.0809793106

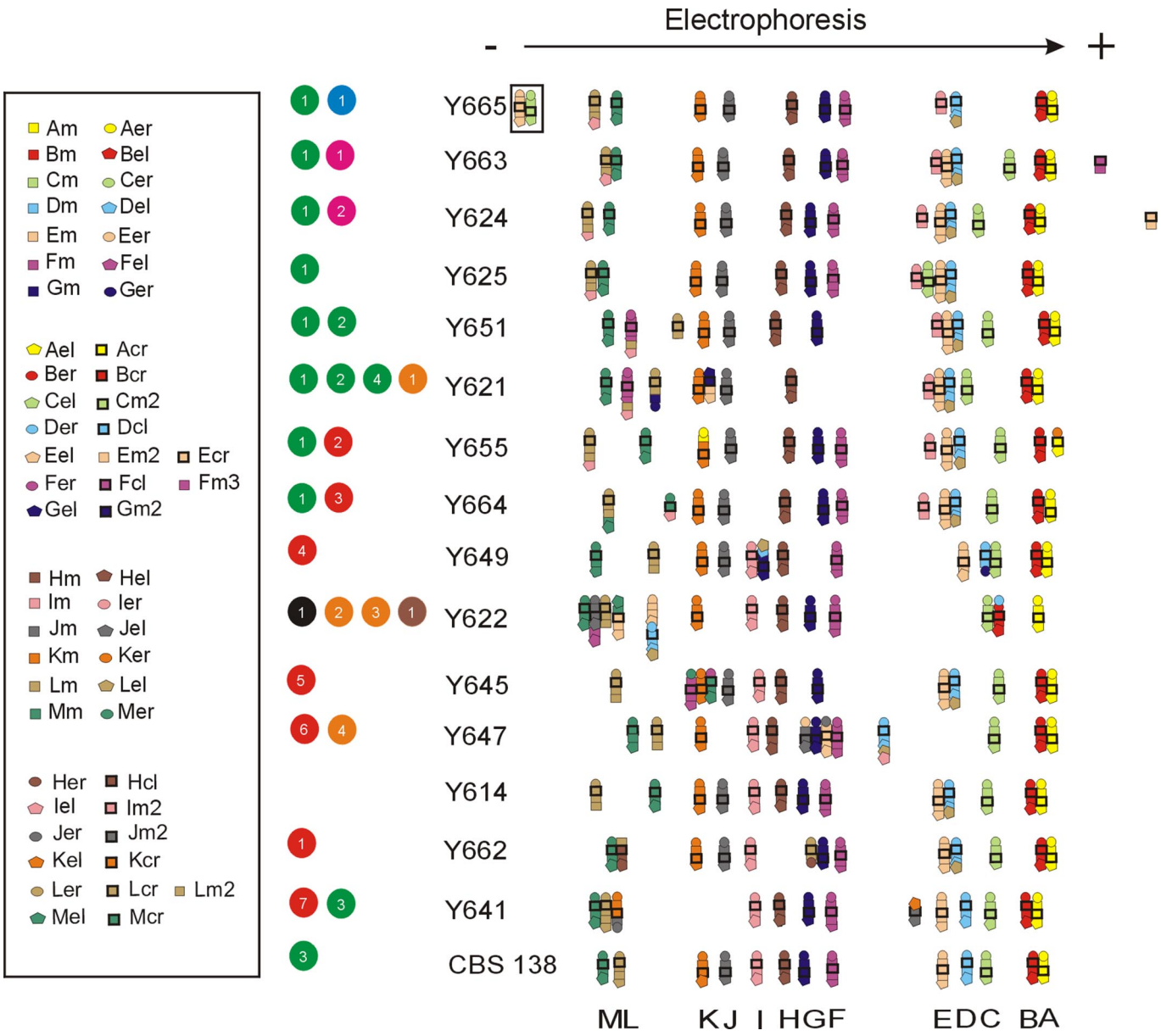

Fig. 1. Electrophoretic karyotypes and detailed mapping of selected *C. glabrata* clinical isolates. A minimum of 4 probes labeled with the same color were used per chromosome: 1 or 2 from the middle of the chromosome marked by squares and 2 from the near of the chromosome ends, left marked by pentagons and right marked by circles, and 1 from close to the centromere marked with a bold black square (for details see Tables S3 and S4 and Fig. S1). Using CBS 138 as the standard, the obtained results can be explained as 7 reciprocal translocations (RT), marked by red circles: event 1, reciprocal translocation between the right arm of chromosome H (H_R) and the left arm of chromosome L (L_L) (RT between H_R and L_L); event 2, RT between K_R and A_R; event 3, RT between L_L and M_L; event 4, RT between G_R and D_L; event 5, RT between M_R and F_R; event 6, RT between J_R and E_R; event 7, RT between K_L and J_R and 4 nonreciprocal translocations (NRT), marked by green circles: event 1, translocation of the left arm of chromosome I (I_L) onto chromosome L (NRT of I_L onto L) (note that NTR of L onto I is equally probable in the common ancestor of all of the strains from Y650 down to CBS 138, see Fig. S2 and Fig. 2); event 2, NRT of L_L onto F; event 3, NRT of D onto L (in all strains but Y641, CBS 138 chromosome D has a different configuration, therefore it is likely that CBS 138 chromosome D originated in this branch by a translocation event); event 4, NRT of G_R onto L. Also several segmental duplications can be observed and are divided into different classes (9). Class III duplications are marked by orange circles, and class II are marked by brown circles. Class III: event 1, interchromosomal duplication (ID) of the left chromosomal arm of chromosome E (E_L) and its translocation onto chromosome G (ID of E_L onto G); event 2, ID of D_R onto B; event 3, ID of F_L onto J; event 4, ID of I_L onto D. Class II: event 1, ID of E_L and M_L (duplication of 2 segments from different chromosomes fused together). The chromosomes E and C in the strain Y665, marked by black square and blue circle, respectively, did not move into the gel in the electrophoretic field. The black circle stands for fusion of chromosome E and D in the strain Y622 and is further explained in Fig. 3. Appearance of a novel chromosome is marked by pink circles, encompassing a segment from chromosome F event 1 and encompassing a segment from the chromosome E event 2.

were observed. The duplicated segments ranged in size from 40 to 700 kb, which is similar to the previously observed *Saccharomyces cerevisiae* duplications generated during growth under laboratory conditions (9). However, one should note that the observed *C. glabrata* duplications were characterized in the "native" isolates.

The comparison of chromosomal rearrangements and phylogenetic relationships positioned the origins of the observed rearrangement events to specific branches of the phylogenetic tree (Fig. 2). Only in a single case did similar translocations not cluster together on the phylogenetic tree; the translocations between chromosome M and F in isolates Y645 and Y650 may

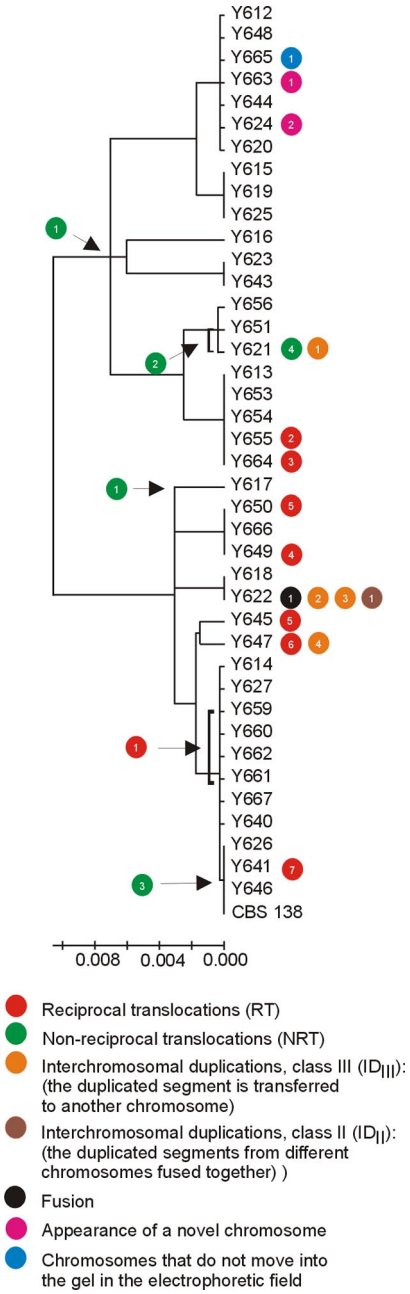

Fig. 2. Chromosomal rearrangements and phylogenetic relationship among 41 *C. glabrata* clinical isolates. The tree is based on the IGS region between CAGL0A00605g and CAGL0A00627g on chromosome A, and the scale bars represent the number of base substitutions per site. Specific events are placed on the phylogenetic tree. The symbols illustrating chromosome changes are as in Fig. 1.

represent independent events. It is noteworthy that even isolates having the identical intergenic sequences showed chromosomal reorganizations, suggesting a high frequency of chromosome remodeling events. For example, Y649, Y650, and Y666 belong to the same phylogenetic cluster but have undergone different chromosomal rearrangements (Fig. 2).

Novel Chromosomes. Although in a majority of strains we found 13 chromosomes, 2 isolates, Y624 and Y663, exhibited 14 (Figs. 1 and 3). The novel chromosomes are small and seem to be composed of a large 120- to 200-kb segmental duplication that carries the centromere region. In Y624, the novel 120-kb chromosome contains a partial duplication of chromosome E with a subsequent deletion of 40–60 kb (Fig. 3*A* and Fig. S3*A*). In Y663, the novel 200-kb chromosome is a partial duplication of chromosome F (Fig. 3*B* and S3*B*). These new chromosomes appear to have acquired telomeres. An oligonucleotide mimicking the *C. glabrata* telomeric repeat gave a clear and specific Southern analysis signal with the 2 small chromosomes, indicating that the most terminal chromosome parts have a structure similar to other chromosomes (Fig. 4). As described in *S. cerevisiae* (10), when a segment containing an active centromere is duplicated, DNA ends can acquire telomeres by initiating a recombination-dependent DNA replication. Apparently, *C. glabrata* also possesses an effective mechanism to "add" viable chromosome ends.

In addition to de novo chromosome generation, we observed chromosome fusions. For example, Y622 carries 2 chimeric chromosomes, a fusion of chromosomes D and E, and a fusion of parts of chromosome E and M (Fig. 3 *C* and *D* and Fig. S4*A*). The original chromosome E is missing from the isolate. A 50- to 80-kb region carrying the chromosome E centromere is deleted from the chromosome D + E chimera. However, these sequences are present in the chromosome E + M chimera. Because the segment of chromosome E in this chimera is larger than the segment deleted from the chromosome D + E chimera, it is likely that the chromosome E segment was duplicated and translocated to chromosome M before the chromosome E centromere was deleted from the chromosome D + E chimera. These structures of these novel fusion chromosomes show that it is important that the chimeric chromosomes contain a single active centromere so as not to destabilize chromosome partitioning during mitosis (11). Surprisingly, Y665 showed only 11 chromosomal bands (Fig. 1). However, the probes specific for the chromosome E and C genes hybridized to the loading well, indicating that these 2 chromosomes adopted a structure that does not allow them to move into the gel. Chromosome circularization, observed in other yeasts (12), could explain such a retarded movement in the electrophoretic field.

Another interesting aspect of the novel chromosomes are their breakage points (Table S5). *C. glabrata* does not posses the major repeat sequences, like *Candida albicans*, and transposons, like *S. cerevisiae* (4). However, several classes of mini- and mega-satellites have been found (13), and two of them coincide with the internal deletions of the Y624 minichromosome (Fig. 3*A* and Fig. S4*C*) and the Y622 fusion chromosome D+E (Fig. 3*C* and Fig. S4*A*). In addition, some of the observed breakpoints correlate with the regions, which were involved in the "historical" rearrangements taking place during the evolution of Hemiascomycetes (Figs. S3 and S4).

Our *C. glabrata* isolates with segmental aneuploidy and extra chromosomes did not exhibit any significant delay in cell proliferation when compared with other isolates. However, the genetic stability of the novel chromosomes was decreased. When *C. glabrata* Y624 and Y663, carrying extra chromosomes, were grown in liquid yeast extract/peptone/dextrose (YPD) medium for 70 generations, a number of the resulting cells lost the extra chromosome (Fig. 5). The loss was observed in 40% of the resulting progeny originating from Y624 and in 70% of the progeny derived from Y663. Is there any advantage then to keeping the duplicated regions and novel chromosomes?

Duplicated Genes. Aneuploidy by gain of small chromosomes or segmental aneuploidy were the most prevalent events on the left arm of chromosome E ($chrE_L$, 3 events of 8) and the left arm of chromosome F ($chrF_L$, 2 events of 8) (Fig. 1). Several genes on $chrE_L$ and $chrF_L$ potentially play a role in *C. glabrata* interaction with the host. Both duplicated segments of $ChrF_L$ encode a transporter of the ATP-binding cassette family (CAGL0F01419g) that is highly similar to *S. cerevisiae AUS1*. The small chromosome

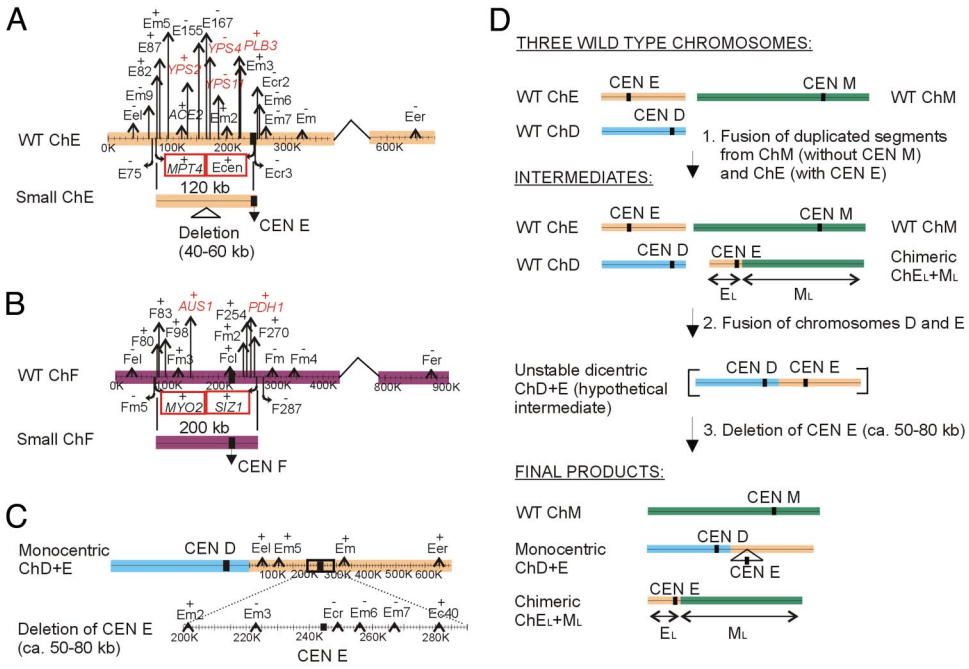

Fig. 3. Segmental duplications involved in the origin of novel chromosomes. (*A*) Y624 carries a duplication of chromosome E corresponding to a ≈120-kb fragment, which has subsequently deleted a 40- to 60-kb segment. (*B*) Y663 carries a duplication of chromosome F corresponding to ≈200 kb. Black stripes symbolize the position of centromeres (CEN). WT stands for CBS 138 chromosome architecture. The last genes identified as present on the novel chromosomes are marked by red squares. The previously described genes involved in virulence or drug resistance are marked in red. (*C*) CBS 138 chromosome D and E fusion found in Y622. Note a large deletion in the CEN E region. (*D*) A model illustrating the origin of the chromosome D and E fusion found in Y622. The centromere (CEN) of the original chromosome E (ChE) was removed by a deletion of a ≈50- to 80-kb region, thereby eliminating a dicentric chromosome structure. The deleted region also covering centromere E was retained on chimeric chromosome composed of the left arm of chromosome E and the left arm of chromosome M. The centromere E fragment in the chimeric chromosome is of a larger size as the region deleted around centromere E in the monocentric D plus E chromosome.

F encodes an ortholog of *S. cerevisiae* ABC transporter *PDR5* (CAGL0F02717g) known in *C. glabrata* as *PDH1*. Its paralog, known as *CDR1* (CAGL0M01760g), is present on chromosome M and was found duplicated in Y622. ABC transporters are implicated in pleiotropic drug resistance, and therefore the duplications could increase the level of drug resistance. Inspection of the chrE_L arm showed that the 3 duplicated segments, in Y621, Y622, and Y624, encode the cluster of the *S. cerevisiae YPS* orthologs coding for extracellular glycosyl phosphatidylinositol-linked aspartyl proteases (CAGL0E01419g, CAGL0E01727g, CAGL0E01749g, CAGL0E01771g, CAGL0E01793g, CAGL0E01815g, CAGL0E01837g, CAGL0E01859g, CAGL0E01881g) and an ortholog of *PLB3* encoding phospholipase B (CAGL0E02321g). The novel chromosome in Y624 has deleted a large part of this region but kept *YPS2* (CAGL0E01419g) encoding a protease and *PLB3* (CAGL0E02321g) encoding a phospholipase B. Secreted aspartyl proteases and a phospholipase B have been shown to play an important role in *C. albicans* virulence (14–16). Recently, Kaur *et al.* (17) have shown that in *C. glabrata* the aspartyl protease-encoding genes are required for survival in macrophages.

In *C. albicans* an aneuploidy and a specific segmental aneuploidy, consisting of an isochromosome composed of 2 left arms of chromosome 5, have been found to occur in response to antifungal drug selection (18). Increases and decreases in drug resistance were strongly associated with gain and loss of this isochromosome that bears genes involved in azole drug resistance. In *C. glabrata*, the original isolate of Y663 carrying the minichromosome could tolerate 129.6 mg/L of fluconazole (Table S1). The Y663 clones, which lost the minichromosome (Fig. 5) could only tolerate 14.4 mg/L of fluconazole. In addition, when Y663 was grown in YPD in the presence of azole (at a concentration of 40 mg/L) for 70 generations, all resulting progeny still kept the extra minichromosomes, whereas in the absence of azole, the loss of minichromosome was observed in 70% of the progeny, indicating that the extra chromosome F confers a growth advantage in the presence of the drug. Apparently, the increase and decrease in gene dosage is a strategy used by *C. glabrata* to overcome environmental pressure, such as the presence of antifungal agents. The observed variable genome structure in the examined pathogenic isolates is therefore an adaptation on the different environmental conditions provided by each individual patient and his/her therapeutic regime.

***C. glabrata* Genome Is Very Dynamic.** It was recently reported by Torres *et al.* (19) that aneuploidy in *S. cerevisiae* is associated with a proliferative disadvantage. However, in *C. glabrata*, segmental duplications, chromosomal rearrangements, and extra chromosomes occur and persist at high frequency.

The high occurrence of certain chromosome events in *C. glabrata*, i.e., chromosome fusions, possible circularizations, non-reciprocal translocations, and novel chromosomes, suggests some sort of telomere dysfunction. So far, 3 telomeric proteins (Rap1, Sir3, Rif1) involved in transcriptional silencing have been analyzed in *C. glabrata* (20, 21). Our inspection of the sequenced *C. glabrata* genome shows that homologues of *S. cerevisiae TEN1* and *RIF2* are missing. The 2 proteins function in telomere end protection and length regulation (22, 23). Notably, deletion of *RIF2* in *S. cerevisiae* leads to recombination-dependent, telomerase-independent telomere elongation (24).

The observed genome dynamics in *C. glabrata* has in general not been seen in other yeasts, except in some mutant backgrounds. However, in certain parasitic protozoa, such as *Leishmania*, a great variation in karyotypes has been reported, and in addition, aneuploidy, gene amplification, and deletion have been reported to be associated with changes in the drug resistance and virulence (25, 26). Elevated chromosome dynamics is not compatible with sexual lifestyle and meiosis but beneficial for adaptation to changing

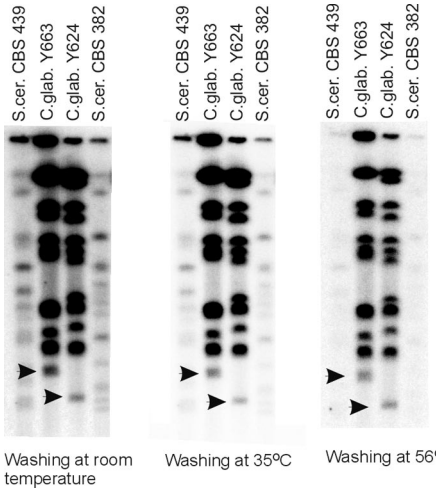

Fig. 4. Hybridization of *C. glabrata* telomeric oligonucleotide (32-mer containing 2 16-bp telomere repeats) to separated chromosomes of 2 *S. cerevisiae* strains (CBS 439 and CBS 382) and 2 *C. glabrata* strains containing extra chromosomes (Y663 and Y624; see also Fig. 1). Hybridization was performed at room temperature, and the membranes were washed at indicated temperatures. Black arrows indicate the positions of the 2 novel chromosomes. Note that the 2 chromosomes hybridized to the telomeric probe even at the most stringent washing conditions. A slightly weaker hybridization signal from small chromosomes is caused by their instability during the propagation (in other words, the mini-chromosomes are not present at the stochiometrical concentration).

environmental conditions. Apparently, *C. glabrata* has to "sacrifice" its sexual nature to better tolerate the consequences of the enhanced genome mutability. The observed elevated adaptability potential should well be taken into account when developing future drugs against this increasingly invasive human pathogen.

Materials and Methods

Yeast Strains. The isolates of *C. glabrata* originate from Danish patients, were collected at Danish hospitals from 1986 to 1999, and were initially identified by carbon assimilation tests (27). The clinical isolates used in this study were randomly selected from a collection of ≈250 isolates (see also ref. 28 and Table S1). The yeast strains were grown at 25 °C in YPD medium consisting of 1% yeast extract, 1% Bacto Peptone, and 2% glucose and in the minimal medium (SD) consisting of 0.17% YNB (yeast nitrogen base without amino acids and without ammonium sulfate), 0.5% ammonium sulfate, and 2% dextrose.

PCR and Sequencing of PCR Products. Genomic DNA was extracted according to Philippsen *et al.* (29). Two regions, nuclear 26S ribosomal RNA coding D1/D2 domain and the mitochondrial small rRNA (*SSU*), were analyzed to confirm the species identity. The D1/D2 domain of the nuclear 26rDNA (*LSU* rDNA) was amplified with primers NL1 (5′P-GCA TAT CAA TAA GCG GAG GAA AAG-3′P) and NL4 (5′P-GGT CCG TGT TTC AAG ACG G-3′P). In the case of the mitochondrial small rRNA (*SSU*), YM5 (5′P-AAG AAT ATG ATG TTG GTT CAG A-3′P) and YM13 (5′P-ATT CTA CGG ATC CTT TAA ACC A-3′P) primers were used. Two primers (NL1, NL4) were used to sequence the D1/D2 domain and 2 primers (YM5, YM13) were used to sequence the mitochondrial *SSU* gene.

The IGS region between the nuclear CAGL0A00605g and CAGLA00627g genes on chromosome A was amplified with primers 00605 (5′P-C TCA CAA ATG GAT TCC TTA AAG AGT TCG-3′P) and 00627 (5′P-GT C ACC AGA GTT GGA GTA CAT GTA G-3′P), and the following conditions were applied: 94 °C initial denaturation for 3 min, then 35 cycles of 45 s at 94 °C, 1 min at 52 °C, and 1 min at 72 °C, followed by 72 °C for 5 min (1 cycle). The IGS region (CAGL0A00605g–CAGL0A00627g) comprising 690 bases was sequenced with primers 00605 and 00627 by MWG Biotech.

The DNA probes (see Fig. S1 and Table S3) for Southern blot analyses were obtained by PCR amplification using *C. glabrata* CBS 138 genomic DNA as a template. PCR conditions for all probes were 94 °C initial denaturation for 3 min, then 35 cycles of 45 s at 94 °C, 45 s at 56 °C, and 1 min at 72 °C, followed by 72 °C for 5 min (1 cycle).

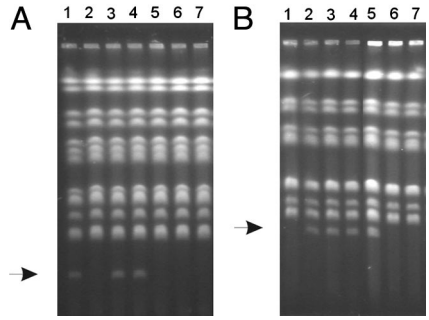

Fig. 5. Chromosome loss in Y624 and Y663 grown in YPD for 70 generations. (*A*) Karyotypes of the parental Y624 strain (line 1) and 6 randomly selected progeny cell lineages (lines 2–7). The position of the small chromosome is indicated by an arrow. (*B*) Karyotypes of the parental strain Y663 (line 2) and 6 randomly selected progeny lineages (lines 1 and 3–7). The position of the small chromosomes is indicated by an arrow.

Phylogenetic Relationships. The sequences of the IGS region were aligned by using the ClustalX (1.83) program (30), and the relationship was inferred by using the neighbor-joining method (31). The phylogenetic tree was linearized assuming equal evolutionary rates in all lineages (32). The tree is drawn to scale, with branch lengths in the same units as those of the evolutionary distances used to infer the phylogenetic tree. The evolutionary distances were computed by using the Maximum Composite Likelihood method (33) and are in the units of the number of base substitutions per site. All positions containing gaps and missing data were eliminated from the dataset (Complete deletion option). There were a total of 671 positions in the final dataset. Phylogenetic analyses were constructed in MEGA4 (34).

PFGE and Southern Hybridization. Chromosomes of all clinical isolates were separated by PFGE using a CHEF Mapper XA (Bio-Rad) and a 5-step program, as follows: step 1, 240-s pulse for 6 h; step 2, 160-s pulse for 13 h; step 3, 120-s pulse for 10 h; step 4, 90-s pulse for 10 h; and step 5, 60-s pulse for 3 h. The included angle was 60° and the voltage was 150 V (4.5 V/cm). Chromosomes and membranes were prepared as described (35). ORF DNA on the membrane was detected by Southern blot analysis using ^{32}P-labeled PCR products as probes (GE Healthcare) (Fig. S1 and Table S3). After prehybridization, the membrane was hybridized (0.25 M Na_2HPO_4, 7% SDS, 1 mM EDTA) at 60 °C for 15 h and washed twice at room temperature for 5 min and once at 60 °C for 30 min with 2% SDS, 100 mM Na_2HPO_4. The membrane was stripped by using the hot SDS procedure protocol (GE Healthcare) and rehybridized more than once. Signals were detected by using Imaging Screen-K (35 × 43 cm; Bio-Rad) and Personal Molecular Imager FX (Bio-Rad). We used 93 single-gene probes and 1 multigene probe to detect and analyze the chromosomal rearrangements.

In the case of the telomeric probe, the 5′ end of the telomeric oligonucleotide sequence (32-mer containing 2 16-bp telomere repeats, TCTGGGTGCT-GTGGGGTCTGGGTGCTGTGGGG) was labeled with [γ^{32}P]-ATP with T4 polynucleotide kinase (Abgene). The membrane was prehybridized and hybridized at room temperature and washed at different temperature stringencies for 30 min.

Batch Culture Growth and Chromosome Stability. All clinical isolates and *C. glabrata* CBS 138 strain were grown in 50 mL of YPD at 25 °C to OD_{600} = 10. Cultures were inoculated with 120 μL of overnight culture, and OD_{600} was measured every 3 h to determine the cell doubling time.

To study instability of extra chromosomes the strains Y624 and Y663 were first plated on YPD medium to isolate single colonies. The single colonies were analyzed by PFGE to confirm the aneuploidy. Three independent aneuploid single colonies from each isolate were inoculated in 2 mL of YPD and cultivated for 70 generations at 25 °C. Every day the cultures were reinoculated, and 2 μL of the old culture was transferred into new liquid YPD. Finally, 14 single colonies were checked by PFGE for loss of the extra chromosomes. To determine the doubling time, 3 single colonies with and 3 single colonies without extra chromosome were grown in 50 mL of SD medium at 25 °C to OD_{600} = 7. Cultures were inoculated with 120 μL of overnight culture, and OD_{600} was measured every 3 h.

Antifungal Drugs. Fluconazole susceptibility was measured on RPMI medium 1640 agar plates (0.84% RPMI medium 1640 with L-glutamine and no bicarbonate, 3.45% Mops, 2% glucose, 1.5% bacto agar adjusted to pH 7 with 1 M NaOH) with 6 different concentrations of fluconazole (4.8, 14.4, 43.2, 129.6, 388.8, and 1166.4 mg/L). Appropriate 10 times dilutions of each cell suspension

(containing 10, 10^2, and 10^3 cells) were plated on RPMI medium 1640 agar plates. The plates were incubated for 48 h at 37 °C.

In the case of strain Y663, the aneuploid single colonies were additionally grown for 70 generations in YPD + 40 mg/L fluconazole. Every day the cultures were reinoculated by transfer of 2 μL of the old culture into a new liquid YPD + fluconazole. Appropriate dilutions of each individual suspension were plated on YPD, and the 14 resulting single colonies were checked by PFGE for chromosome loss.

ACKNOWLEDGMENTS. We thank Linda Hellborg, Morten Kielland-Brandt, Torsten Nilsson-Tillgren, and Ken Wolfe for comments on the early version of this manuscript and Eimantas Astromskas for technical assistance in some experiments. This work was supported by the Swedish Research Council and the Fysiografen, Crafoord, Lindström, Lawski, and Sörensen Foundations.

1. Gauwerky CE, Croce CM (1993) Chromosomal translocations in leukemia. *Semin Cancer Biol* 4:333–340.
2. Sharpless NE, *et al.* (2001) Impaired nonhomologous end-joining provokes soft tissue sarcomas harboring chromosomal translocations, amplifications, and deletions. *Mol Cell* 8:1187–1196.
3. Delneri D, *et al.* (2003) Engineering evolution to study speciation in yeasts. *Nature* 422:68–72.
4. Dujon B, *et al.* (2004) Genome evolution in yeasts. *Nature* 430:35–44.
5. Klempp-Selb B, Rimek D, Kappe R (2000) Karyotyping of *Candida albicans* and *Candida glabrata* from patients with Candida sepsis. *Mycoses* 43:159–163.
6. Shin JH, *et al.* (2007) Changes in karyotype and azole susceptibility of sequential bloodstream isolates from patients with *Candida glabrata* candidemia. *J Clin Microbiol* 45:2385–2391.
7. Lin CY, Chen YC, Lo HJ, Chen KW, Li SY (2007) Assessment of *Candida glabrata* strain relatedness by pulsed-field gel electrophoresis and multilocus sequence typing. *J Clin Microbiol* 45:2452–2459.
8. Fischer G, James SA, Roberts IN, Oliver SG, Louis EJ (2000) Chromosomal evolution in *Saccharomyces. Nature* 405:451–454.
9. Koszul R, Caburet S, Dujon B, Fischer G (2004) Eukaryotic genome evolution through the spontaneous duplication of large chromosomal segments. *EMBO J* 23:234–243.
10. McEachern MJ, Haber JE (2006) Break-induced replication and recombinational telomere elongation in yeast. *Annu Rev Biochem* 75:111–135.
11. McClintock B (1984) The significance of responses of the genome to challenge. *Science* 226:792–801.
12. Naito T, Matsuura A, Ishikawa F (1998) Circular chromosome formation in a fission yeast mutant defective in two ATM homologues. *Nat Genet* 20:203–206.
13. Thierry A, Bouchier C, Dujon B, Richard GF (2008) Megasatellites: A peculiar class of giant minisatellites in genes involved in cell adhesion and pathogenicity in *Candida glabrata. Nucleic Acids Res* 36:5970–5982.
14. Ghannoum MA (2000) Potential role of phospholipases in virulence and fungal pathogenesis. *Clin Microbiol Rev* 13:122–143.
15. Mukherjee PK, *et al.* (2001) Reintroduction of the *PLB1* gene into *Candida albicans* restores virulence in vivo. *Microbiology* 147:2585–2597.
16. Naglik J, Albrecht A, Bader O, Hube B (2004) *Candida albicans* proteinases and host/pathogen interactions. *Cell Microbiol* 6:915–926.
17. Kaur R, Ma B, Cormack BR (2007) A family of glycosylphosphatidylinositol-linked aspartyl proteases is required for virulence of *Candida glabrata. Proc Natl Acad Sci USA* 104:7628–7633.
18. Selmecki A, Forche A, Berman J (2006) Aneuploidy and isochromosome formation in drug-resistant *Candida albicans. Science* 313:367–370.
19. Torres EM, *et al.* (2007) Effects of aneuploidy on cellular physiology and cell division in haploid yeast. *Science* 317:916–924.
20. Haw R, Yarragudi AD, Uemura H (2001) Isolation of a *Candida glabrata* homologue of *RAP1*, a regulator of transcription and telomere function in *Saccharomyces cerevisiae. Yeast* 18:1277–1284.
21. Castaño I, *et al.* (2005) Telomere length control and transcriptional regulation of subtelomeric adhesins in *Candida glabrata. Mol Microbiol* 55:1246–1258.
22. Wotton D, Shore D (1997) A novel Rap1p-interacting factor, Rif2p, cooperates with Rif1p to regulate telomere length in *Saccharomyces cerevisiae. Genes Dev* 11:748–760.
23. Grandin N, Damon C, Charbonneau M (2001) Ten1 functions in telomere end protection and length regulation in association with Stn1 and Cdc13. *EMBO J* 20:1173–1183.
24. Teng SC, Chang J, McCowan B, Zakian VA (2000) Telomerase-independent lengthening of yeast telomeres occurs by an abrupt Rad50p-dependent, Rif-inhibited recombinational process. *Mol Cell* 6:947–952.
25. Beverley SM (1991) Gene amplification in *Leishmania. Annu Rev Microbiol* 45:417–444.
26. Ubeda JM, *et al.* (2008) Modulation of gene expression in drug-resistant *Leishmania* is associated with gene amplification, gene deletion, and chromosome aneuploidy. *Genome Biol* 9:R115.
27. Wickerham LJ, Burton KA (1948) Carbon assimilation tests for the classification of yeasts. *J Bacteriol* 56:363–371.
28. Mentel M, Spírek M, Jørck-Ramberg D, Piskur J (2006) Transfer of genetic material between pathogenic and food-borne yeasts. *Appl Environ Microbiol* 72:5122–5125.
29. Philippsen P, Stotz A, Scherf C (1991) DNA of *Saccharomyces cerevisiae. Methods Enzymol* 194:169–182.
30. Thompson JD, Gibson TJ, Plewniak F, Jeanmougin F, Higgins DG (1997) The CLUSTALX windows interface: Flexible strategies for multiple sequence alignment aided by quality analysis tools. *Nucleic Acids Res* 25:4876–4882.
31. Saitou N, Nei M (1987) The neighbor-joining method: A new method for reconstructing phylogenetic trees. *Mol Biol Evol* 4:406–425.
32. Takezaki N, Rzhetsky A, Nei M (1995) Phylogenetic test of the molecular clock and linearized trees. *Mol Biol Evol* 12:823–833.
33. Tamura K, Nei M, Kumar S (2004) Prospects for inferring very large phylogenies by using the neighbor-joining method. *Proc Natl Acad Sci USA* 101:11030–11035.
34. Tamura K, Dudley J, Nei M, Kumar S (2007) Molecular Evolutionary Genetics Analysis (MEGA) software version 4.0. *Mol Biol Evol* 24:1596–1599.
35. Petersen RF, Nilsson-Tillgren T, Piskur J (1999) Karyotypes of *Saccharomyces* sensu lato species. *Int J Syst Bacteriol* 49:1925–1931.